

**SPECIAL FEATURE:
TUTORIAL****Fourier Transform Mass Spectrometry****I. Jonathan Amster**

Department of Chemistry, University of Georgia, Athens, GA 30602-2556, USA

The fundamental principles of Fourier transform mass spectrometry (FTMS) are presented. The motion of ions in a FTMS analyzer can be understood in terms of the magnetic and electric fields present in the FTMS analyzer cell. Ion motion is illustrated with the results of ion trajectory calculations under both collision-free conditions and at high pressure. Dipolar and quadrupolar excitation are described and compared. Practical considerations in obtaining ultra-high-mass resolution and accuracy are discussed. The FTMS experiment is a series of events (ionization excitation, detection) that occur in sequence. Pulse sequences for mass spectrometric and tandem mass spectrometric experiments are presented.

KEYWORDS: ion trajectories; quadrupolar excitation; high resolution mass spectrometry

INTRODUCTION

Fourier transform mass spectrometry (FTMS) has received considerable attention for its ability to make mass measurements with a combination of resolution and accuracy that is higher than any other mass spectrometer, most recently for biomolecules ionized by electrospray ionization (ESI)^{1,2} and matrix-assisted laser desorption/ionization (MALDI).^{3,4} It is a versatile instrument that can be adapted to a variety of analytical and physical chemistry measurements. It can be used to obtain high-resolution mass spectra from ions formed by practically every known ionization method,⁵⁻¹⁰ to perform tandem mass spectrometric measurements¹¹⁻¹⁶ and to examine ion chemistry¹⁷⁻²³ and photochemistry.²⁴⁻²⁷ Its versatility follows from the fact that it is an ion trapping instrument, as is the r.f. quadrupole mass spectrometer. The FTMS instrument mass analyzes and detects ions using methods which are unique among mass spectrometers.

Fourier transform mass spectrometry derives from ion cyclotron resonance (ICR) spectrometry. The theory of cyclotron resonance was developed by Lawrence in the 1930s.²⁸ Lawrence built the first cyclotron accelerator, used to study the fundamental properties of the atom. In the 1950s, the principle of ion cyclotron resonance was first incorporated into a mass spectrometer called the omegatron, by Sommer et al.²⁹ Other designs followed over the next 15 years, producing instruments that were used principally to study ion-molecule reactions. In 1978, Comisarow and Marshall adapted Fourier transform methods to ICR spectrometry³⁰ and built the first FTMS instrument.³¹ Since that time, interest in FTMS has increased exponentially, as has the number of FTMS instruments. A number of reviews of FTMS have been written, which cover many of the aspects of the technique and its applications.³²⁻⁴² This

paper will focus on the fundamental principles that underlie FTMS and the practical details necessary to achieve high performance and will provide references for the reader to find current examples of the capabilities of this technique.

APPARATUS

Several types of FTMS instruments can be found in laboratories throughout the world. Many have been built by investigators to perform experiments that demand high performance under a variety of conditions, such as ultra-precise mass measurements of low molecular mass ions⁴³ or high molecular mass ions,⁴⁴ while interfacing sources with supersonic jet expansion,⁴⁵ atmospheric ionization⁴⁶ or laser microprobe capabilities.⁴⁷ All FTMS instruments have in common four main components. First is a magnet, which can be either a permanent magnet, an electromagnet or a superconducting magnet. Permanent magnets have low field strengths that limit the performance of an FTMS instrument and only a few systems have been built with these.⁴⁸ Electromagnets are limited to field strengths below 2 T, although 1 T is most common. At these fields, FTMS instruments are capable of achieving high performance for ions of relatively low mass-to-charge ratio. The performance of the FTMS instrument improves as the magnetic field strength increases and so the trend is to design instruments with stronger fields using superconducting magnets. These are solenoidal magnets with relatively wide bores compared with those used for NMR spectroscopy. The superconducting magnets used for FTMS have field strengths ranging from 3 to 9.4 T. A 20 T resistive magnet has been recently used for demonstration FTMS experiments at the National High Magnetic Field Laboratory,⁴⁹ and

other magnets with field strengths in excess of 12 T are being constructed for FTMS experiments at the NIMFL and at Battelle Pacific Northwest National Laboratory.

The second component common to FTMS instruments is the analyzer cell. The cell is the heart of the FTMS instrument, where ions are stored, mass analyzed and detected. Several analyzer cell designs have been developed. Figure 1 shows two common types of analyzer cells.

The cubic cell was the first type of analyzer used for FTMS and is still widely used today. It is composed of six plates arranged in the shape of a cube. This cell is oriented in the magnetic field so that one opposing pair of plates is orthogonal to the direction of the magnetic field lines and two pair of plates lie parallel to the field. The plates that are perpendicular to the field are called the trapping plates. For the cubic cell shown in Fig. 1, one of the two trapping electrodes is visible and can be identified as the plate with a hole through its center. It is common for trapping electrodes of cubic cells to have openings that permit electrons or ions to enter the cell along the magnetic field lines. The four remaining plates are used for ion excitation and ion detection, as explained below.

Other types of cells have been developed to provide a variety of capabilities. The open-ended cylindrical cell, shown in Fig. 1, differs in appearance from the cubic cell, but has six electrodes that perform the same functions as those of the cubic cell. This cell is oriented so that the principal axis of the cylinder aligns with the magnetic field. The trapping electrodes in this design are the two cylinders at the ends of the cell. The center cylinder is divided into four electrodes that function as excitation and detection plates. This shape and dimensions of this cell make it more suitable to fit into the bore of a superconducting magnet, while the cubic cell is better matched with the narrow gap between the pole caps of an electromagnet. Many other cell designs have been proposed. A recent review presents the relative advantages of several cell types of analyzer cells.⁵⁰

The third feature required of FTMS instruments is an ultra-high vacuum system. While all mass spectrometers require vacuum for the analysis and detection of ions,

the performance of the FTMS instrument is more sensitive to pressure than other instruments. As will be discussed below, high vacuum is required to achieve high resolution. For ultra-high resolution, pressures of 10^{-9} – 10^{-10} Torr (1 Torr = 133.3 Pa) are required. To achieve these low pressures, cryogenic pumps or turbomolecular pumps are used more frequently than diffusion pumps. Low pressure is required only when ions are detected. Ion formation and detection occur at different times in an FTMS experiment, so that these instruments can also operate at elevated pressure for a portion of the experiment, provided that high vacuum is restored during ion detection. Most FTMS vacuum systems are equipped with pulsed valves so that the pressure can be increased for a brief duration, for example to introduce a sample for ion–molecule studies or to collisionally activate trapped ions.

The fourth feature that is shared by all FTMS instruments is a sophisticated data system. Many of the components of the data system are similar to those used for FT-NMR. They include a frequency synthesizer, delay pulse generator, broadband r.f. amplifier and pre-amplifier, a fast transient digitizer and a computer to coordinate all of the electronic devices during the acquisition of data, as well as to process and analyze the data. The tremendous growth and development of the semiconductor industry have benefitted FTMS. Electronics hardware costs for FTMS have remained level over the last decade, while performance has increased dramatically.

ION MOTION

The motion of ions in the FTMS analyzer cell is governed by the magnetic and electric fields that are present. This is stated concisely in the force expression shown in Eqn (1), in which \mathbf{F} is the sum of the forces that act upon an ion of charge q and velocity \mathbf{v} arising from its interaction with the electric field \mathbf{E} and from its interaction with the magnetic field \mathbf{B} . The magnetic field is uniform, unidirectional and homogeneous and so the value of \mathbf{B} in Eqn (1) is a constant in the volume of the analyzer cell and, in addition, is constant over time. The electric field principally arises from the voltages that are applied to the electrodes of the analyzer cell and can have both r.f. and d.c. components. To a lesser degree, the electric field is also influenced by the ions themselves. As with all mass spectrometers, at high ion densities, space charge can perturb the desired behavior of the ions and adversely affect the performance of the instrument. The magnitude of space charge perturbations depends on the density of the ions, the strength of the magnetic field, the m/q ratio of the ions and the dimensions of the analyzer cell. At low ion densities, space charge causes small changes in the apparent mass of the ions.^{51–53} At higher densities, Coulomb broadening of the peaks arises,⁵⁴ and relative peak heights can be perturbed.⁵⁵ At even higher ion densities, peak coalescence occurs, which is described later. Above the space-charge limit of an analyzer cell, roughly 10^7 charges, ions are lost from the cell.

$$\mathbf{F} = q\mathbf{E} + q(\mathbf{v} \otimes \mathbf{B}) \quad (1)$$

Cyclotron Motion Ion in a Magnetic Field

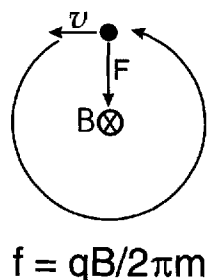
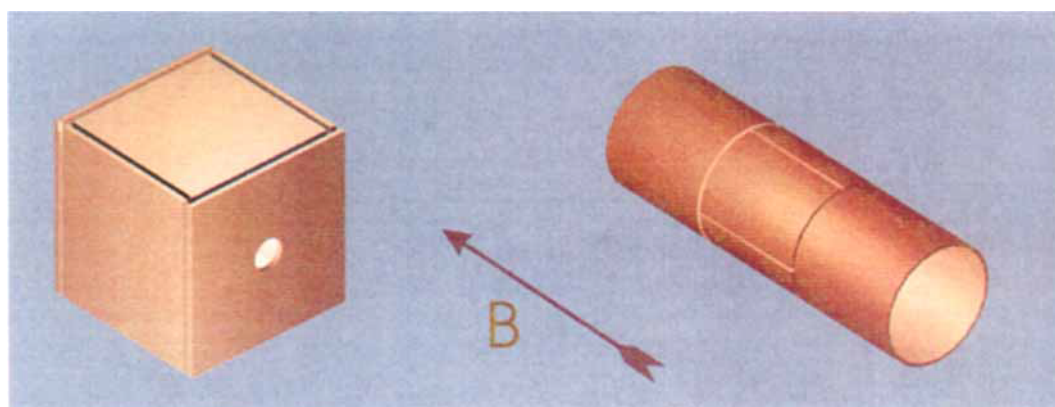


Figure 2. Cyclotron motion in the plane perpendicular to the magnetic field lines. The magnetic field is pointing into the plane of the page. An ion moving to the left experiences a downward force that drives it into a counterclockwise orbit.

FTMS Analyzer Cells



Cubic Cell

Cylindrical Open-Ended

Figure 1. A cubic analyzer cell and a cylindrical, open-ended cell for FTMS. The arrow shows the orientation of the magnetic field lines. The functions performed by the individual electrodes are described in the text.

Cyclotron motion

The basis for FTMS is ion cyclotron motion, which arises from the interaction of an ion with the unidirectional magnetic field. The magnetic field acts on the component of an ion's velocity that is perpendicular to the magnetic field axis, as indicated by the cross product term in Eqn (1). An ion experiences a force that is perpendicular to both the direction of its velocity and the magnetic field. This force, called the Lorentz force, causes an ion to travel in a circular orbit that is perpendicular to the magnetic field, as shown in Fig. 2. Cyclotron motion is periodic and is characterized by its cyclotron frequency, that is, the frequency with which an ion repeats its orbit. The cyclotron frequency is determined by only three physical parameters, the strength of the magnetic field, B , the charge present on an ion, q , and the mass of the ion, m , as shown by Eqn (2). Cyclotron frequencies fall in the range of tens of kilohertz to megahertz. For example, at 7 T an ion of m/q 1000 will have a cyclotron frequency of 107.4 kHz ($1.602 \times 10^{-19} \text{C} \times 7.000 \text{T} / 2 \times \pi \times 1000 \text{u} \times 1.673 \times 10^{-27} \text{kg u}^{-1}$).

$$f_c = \frac{qB}{2\pi m} \quad (2)$$

In FTMS, the magnetic field is held constant and the mass-to-charge ratio of an ion (m/q) is determined by measuring its cyclotron frequency. The simplicity of the governing equation for ion motion in the FTMS instrument is unique among mass spectrometers. In particular, it should be noted that the cyclotron frequency of an ion is independent of its velocity and therefore independent of its kinetic energy. With most other mass spectrometers, an ion's kinetic energy exerts a profound influence on mass analysis. For example, the mass resolution that can be achieved by magnetic sector or time-of-flight mass spectrometers is limited by the spread in the ions' kinetic energy distribution. The insensitivity of the cyclotron frequency to the kinetic energy of an ion is one of the fundamental reasons why

the FTMS instrument is able to achieve ultra-high resolution.

The radius of the cyclotron orbit depends upon the kinetic energy of the ion. An ion's angular frequency, related to the cyclotron frequency of Eqn (2) by a factor of 2π ($\omega_c = 2\pi f_c$), is by definition equal to the ratio of velocity to orbital radius, as in Eqn (3). Since the cyclotron frequency is constant for an ion of given mass-to-charge ratio, the radius of the cyclotron orbit scales directly with an ion's velocity, or with the square root of kinetic energy. Typically, ions that have thermal kinetic energies will have cyclotron radii on the order of 100 μm . As will be shown below, the kinetic energies of the ions are increased in order to detect them and the radius of the cyclotron orbit is increased to a significant fraction of the dimensions of the analyzer cell.

$$\omega_c = \frac{v}{r} \quad (3)$$

Trapping motion

An ion that moves parallel to the magnetic field experiences no force from the field. Thus ion motion along the magnetic field axis is unconstrained. Early ion cyclotron resonance spectrometers used drift cells to detect ions. These were analyzers that allowed a continuous beam of ions to pass through the detection region. The residence time of an ion in an analyzer cell without any trapping electric fields is of the order of milliseconds. In 1970, McIver⁵⁶ introduced the cubic trapped cell to ICR spectrometry. Two plates are mounted perpendicular to the magnetic field to create a potential well that traps ions in the cubic analyzer cell. A small, symmetric positive voltage applied to the trapping plates stores positive ions, while a small negative voltage traps negative ions. Ions undergo simple harmonic oscillation between the trapping plates along the magnetic field axis.

Magnetron motion

The combination of the magnetic and electric fields creates a three-dimensional ion trap. This allows ions to be stored in the ICR analyzer cell for seconds, minutes or even hours, which is many orders of magnitude longer than the residence time of ions in most other types of mass spectrometers. Trapping motion and cyclotron motion are not coupled. Thus it would seem that the electric and magnetic fields operate on the ions in independent fashion. However, the combination of the magnetic and electric field together introduce a third fundamental motion of the ions, called magnetron motion. To understand this, it is necessary to consider the shape of the electric field in the analyzer cell. For the purpose of discussion, let us define a rectangular coordinate system where the origin is the center of the analyzer cell and the z-axis lies parallel to the magnetic field. The magnetic field constrains ion motion in the xy-plane, perpendicular to the z-axis. The trapping potential constrains ion motion along the z-axis.

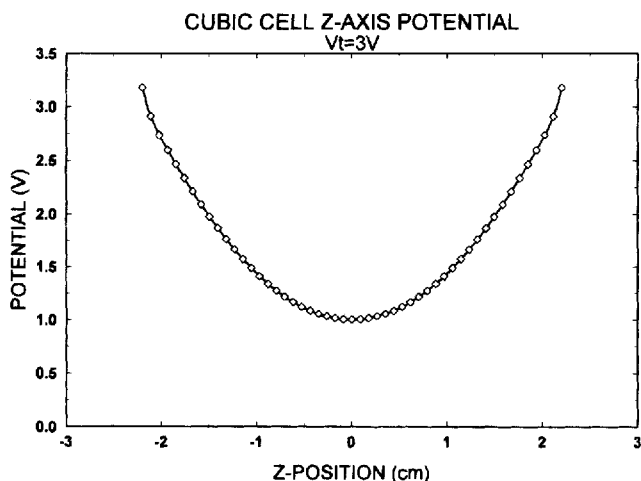


Figure 3. A plot of the electric potential due to the trapping voltage in a cubic cell along the principal axis that lies parallel to the magnetic field, the z-axis. The potential at the center of the cell is one-third of the trapping voltage.

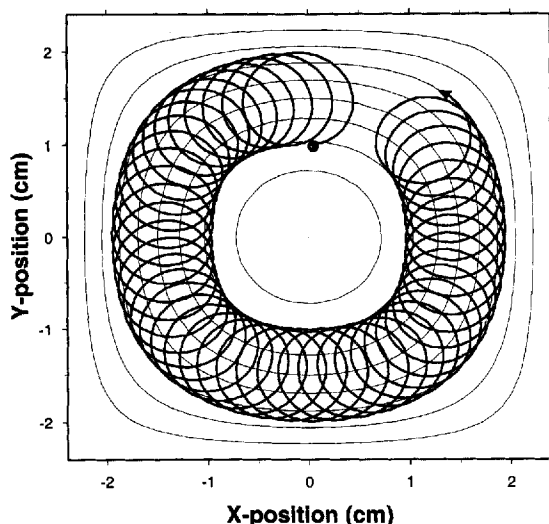


Figure 5. An ion trajectory that shows both cyclotron and magnetron motion plotted on the isopotential contours that result from the trapping voltage. The trajectory is for an ion of m/q 500 with 2 eV of kinetic energy in the xy -plane in a 4.4 cm cubic cell with a 3 V trapping potential at 1 T magnetic field strength. Magnetron motion causes the guiding center of the cyclotron motion to precess around the cell along one isopotential contour. The ion's trajectory begins at the coordinates (0, 1) and ends at (1.2, 1.5). This trajectory shows ion motion in the absence of a collision gas.

The magnitude of the electric potential along the magnetic field axis is plotted in Fig. 3. The potential reaches a maximum at the trapping plates and has a minimum at the center of the cell. Significantly, the trapping potential at the center of the cell is not zero, but is the arithmetic average of the d.c. voltages applied to the six plates of the cubic cell. The four plates that constitute the detection and excitation electrodes are held at ground potential and the two trapping plates receive the full trapping potential and therefore the potential at the center of the cell is one third of the applied trapping voltage $[(2V_t + 4 \times 0)/6 = V_t/3]$. The

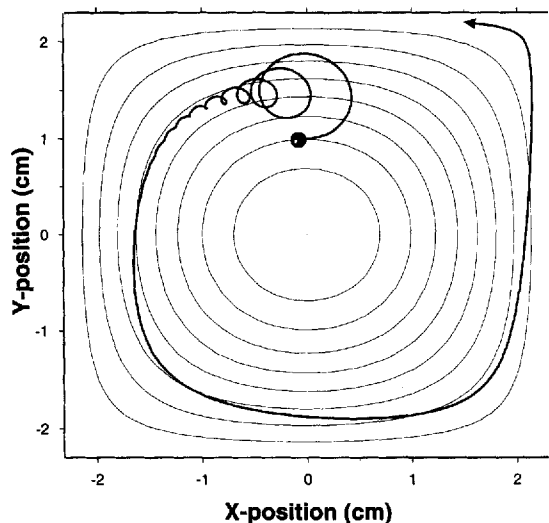


Figure 6. Effect of a collision gas upon ion motion. The initial conditions for the ion are the same as in Fig. 5, but a collision gas is present at a pressure of 0.01 Torr. Cyclotron motion is seen to damp quickly with a collapse of the cyclotron orbit, while the magnetron radius increases as motion in this coordinate slowly damps.

shape of the trapping potential provides a restoring force that traps ions along the z -coordinate, but repels ions in the xy -plane. This can be seen in Fig. 4, which displays a plot of the electrical potential in the xy -plane through the center of the cell. The potential surface is seen to be radially repulsive; the electric field acts to drive ions away from the center of the analyzer cell. The magnetic field prevents ions from being accelerated into the walls of the analyzer cell. The electric and magnetic fields combine to produce magnetron motion, a precession of the guiding center of the cyclotron motion of an ion around the center of the cell.

Figure 5 shows the magnetron and cyclotron motions of an ion in a cubic cell. The plot is an ion trajectory that is calculated by performing numerical integration of the differential form of Eqn (1). For this illustration, the relative magnitude of the magnetron radius to the cyclotron radius is greatly exaggerated compared with normal operating conditions. When detecting ions, the radius of the cyclotron motion of an ion is usually much larger than that of its magnetron component. The magnetron radius of an ion is determined by its initial displacement from the principal axis of the cell when it is formed or injected into the cell. To obtain the best resolution and mass accuracy, the magnetron radius is minimized by creating or injecting ions along the principal axis of the cell that lies parallel to the magnetic field.

Magnetron frequencies are of the order of 1–100 Hz and are much lower than cyclotron frequencies, which fall in the range 5 kHz–5 MHz. Magnetron frequency, f_m , is a function of the magnitude of the trapping potential, V , the magnetic field strength, B , the distance between the trapping plates, a , and the geometry factor α (1.39 for a cubic cell), as shown in Eqn (4). Magnetron frequency is independent of the mass-to-charge ratio of an ion. It should be noted that magnetron motion serves no useful analytical purpose. It is a consequence of the curvature of the trapping electric field due to the finite length of the cell electrodes. The trapping electric field is required to store ions in the cell during analysis, but it exerts adverse effects on ion behavior and mass measurement accuracy. These undesirable effects include radial ion diffusion, described below, mass shifts and sidebands.

$$f_m = \frac{\alpha V}{\pi a^2 B} \quad (4)$$

Effects of collisions

The discussion of ion motion has focused on behavior under collision-free conditions. When ions are detected, the vacuum system of a FTMS instrument is typically maintained at a pressure of 10^{-9} Torr or lower so that collisions happen infrequently. For a variety of experiments, the pressure of the FTMS instrument may be raised, sometimes by several orders of magnitude. Under these conditions, collisions will occur between ions and neutral molecules, which cause a decrease in the kinetic energy of the ions and therefore a reduction of their velocity. The trapping oscillation of ions along the z -axis is damped by collisions, causing the ion cloud

CELL POTENTIAL PLOT IN THE XY-PLANE CUBIT CELL. V_t+3V

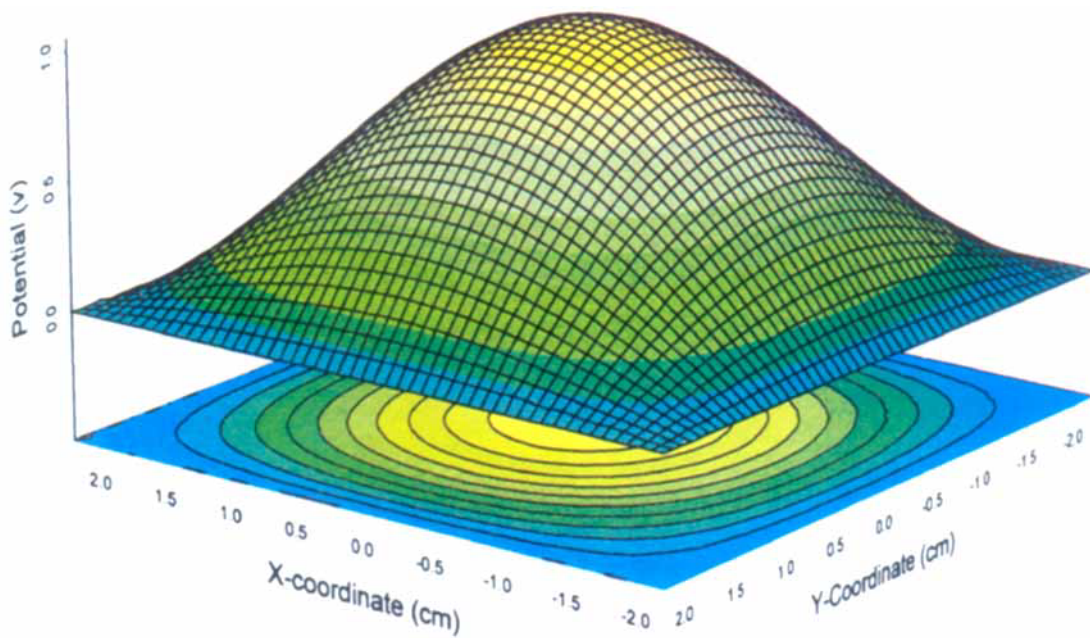


Figure 4. Plot of the electric potential due to the trapping voltage in a cubic cell in the plane that lies perpendicular to the magnetic field, and that passes through the center of the cell. The potential has its maximum in the center of the cell, producing an outward-directed force on ions.

to condense to the center plane of the cell. Collisions also affect the cyclotron motion of ions. As collisions reduce the velocity of an ion, the radius of the cyclotron orbit also decreases, as expected from Eqn (3). In contrast, the magnetron radius expands as collisions allow ions to roll down the "hill" of the potential surface shown in Fig. 3. The potential minimum for the electric field is the edge of the cell in the *xy*-plane. With collisions, ions drift away from the center of the cell and ultimately are lost to neutralizing collisions with the excitation and detection electrodes, a process called collisionally mediated radial diffusion.

An ion trajectory that illustrates the collisional damping of cyclotron and magnetron motions is shown in Fig. 6. Cyclotron motion is seen to damp more rapidly than magnetron motion. The rate of ion loss by radial diffusion depends on the ratio of the trapping voltage to the square of the magnetic field strength. This process limits the number of collisions that an ion undergoes before being lost from the cell when trapped as described above. Other techniques can be used to trap ions while they undergo an infinite number of collisions and these will be described below.^{57,58}

EXPERIMENTAL PROCEDURES

Event sequence

The FTMS instrument operates in a very different fashion than most other types of mass spectrometers. With FTMS, the principal functions of ionization, mass analysis and ion detection occur in the same space (the analyzer cell) but are spread out in time, whereas with quadrupole and magnetic sector mass spectrometers, these events occur simultaneously and continuously, but in different parts of the mass spectrometer. FTMS experiments consist of a series of events called an experimental sequence. A simple experimental sequence is composed of four events; quench, ion formation, ion excitation and ion detection, as illustrated in Fig. 7. The quench event is used to empty the analyzer cell of any ions that may be present from a previous experiment. This can be accomplished by applying antisymmetric voltages to the trapping plates, e.g. +10 V to one trapping plate and -10 V to the other. Under these condi-

Basic Experimental Sequence

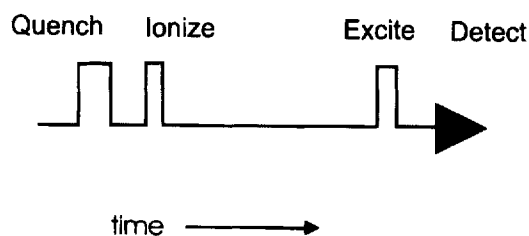


Figure 7. A simple experimental sequence that illustrates the basic steps in obtaining a mass spectrum with FTMS.

tions, ions are axially ejected (along the *z*-axis) from the cell in less than 1 ms. After a short quench event (1–5 ms), a new set of ions is formed and trapped in the cell. Ions can either be formed in the cell, for example by electron impact ionization, or be formed outside the cell and transferred into the cell during the ionization event. Ions may be formed just outside the trapping plates of the analyzer cell by methods that are compatible with ultra-high vacuum, such as MALDI. Ions may also be made outside the magnetic field of the FTMS instrument and guided to the analyzer cell with either electrostatic^{59,60} or r.f. ion lenses.⁶¹ In either of the latter cases, ions that are made outside the trapping field must be transported into the cell and captured by other means, such as gated trapping⁶² or accumulated trapping.^{63,64}

Ion excitation and detection

The next event in the experimental sequence is excitation of the ion's cyclotron motion. After ions are formed and trapped in the analyzer cell, they often have only a small amount of kinetic energy, less than 1 eV. A notable exception occurs for ions that are formed by MALDI, for which the kinetic energy is proportional to the mass of the ion.⁶⁵ In a MALDI experiment, high-mass ions may have tens of electronvolts of kinetic energy. However this energy is usually directed along the *z*-axis and can be reduced by collisional damping. The radius of an ion's cyclotron orbit when first trapped is usually small compared with the dimensions of the cell. In order to detect ions, they are excited into coherent motion by applying a sinusoidal voltage to the excitation plates, an opposing pair of plates which lie parallel to the magnetic field axis. Figure 8 shows the trajectory that results from excitation of an ion at its cyclotron frequency. The ion spirals outwards when its cyclotron frequency is in resonance with the frequency of the applied r.f. electric field. Ions that are not in resonance do not absorb energy and remain at the center of the cell. If the r.f. voltage is applied continuously, the ions that absorb energy will spiral outward until they strike an excitation or detection plate, where they will be neutralized. This feature can be used to remove mass-selected ions from the analyzer cell. If the field is turned off before the ions strike the cell plates, they undergo cyclotron motion, as shown at the bottom of Fig. 8.

All ions of the same mass-to-charge ratio are excited coherently, which means that they are grouped as tightly after excitation as they were initially. Ions of the same mass-to-charge ratio undergo cyclotron motion as a packet. As they pass the cell's electrodes, the coherently orbiting ion packet attracts electrons to first one and then the other of the two detection plates through the external circuit that joins them. (The detection plates, like the excitation plates, are a pair of opposed electrodes which lie parallel to the magnetic axis.) This alternating current is called the image current.⁶⁶ The periodic cyclotron motion of the ions produces a sinusoidal image signal which can be amplified, digitized and stored for processing by a computer. The frequency of the detected sinusoid is nearly equal to the frequency of

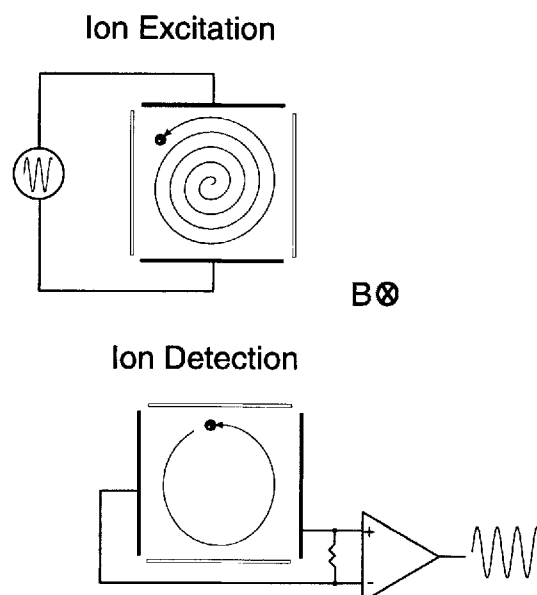


Figure 8. Illustration of dipolar excitation and image current detection for mass analyzing ions in a FTMS analyzer cell. The magnetic field is directed into the plane of the figure. (Top) a sinusoidal voltage is applied to the excitation plates. Ions which are in resonance with the excitation frequency gain kinetic energy and spiral outwards from the center of the cell into a larger cyclotron orbit. (Bottom) after the conclusion of the excitation event, ions continue to undergo cyclotron motion with a large radius orbit. An image signal is produced on the detection plates, which are connected to the amplifier in the figure.

the cyclotron motion of the ions; it is exactly equal to the difference between the cyclotron and magnetron frequencies. Image current detection provides unique capabilities for FTMS. All other mass spectrometers detect ions by destructive collisions with an electron multiplier, although a recent demonstration experiment has shown that image current detection can be achieved in the r.f.-quadrupole ion trap.⁶⁷ Image current detection is non-destructive; the ions remain in the analyzer cell after the detection process has been completed. The significance of this feature will be discussed below.

Ions of many masses can be detected simultaneously with FTMS. To accomplish broadband detection, many frequencies are applied during the excitation event. The most common method for broadband excitation is to use a rapid frequency sweep, or r.f. chirp. For example, a frequency synthesizer can be programmed to sweep over frequencies from 10 kHz to 1 MHz in a 1 ms period. This will cause all ions with cyclotron frequencies in this range to be excited into large cyclotron orbits of the same radius. The image current that results from ions of several mass-to-charge ratios is a composite of sinusoids of different frequencies and amplitudes. An example of the image signal, or transient, that is produced from several different ions is shown on the left side of Fig. 9. The frequency components of the signal are obtained by applying a Fourier transform to the time domain transient. The frequency spectrum is converted into a mass spectrum by applying a calibration formula derived from the cyclotron equation. The image current allows multichannel detection, as can be seen on the right of Fig. 9. In this case, a 1.2 s transient yielded signals for seven groups of ions (seven charge states of

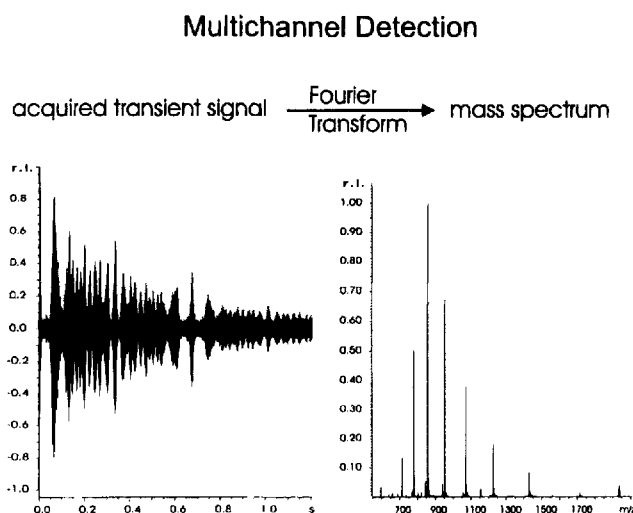


Figure 9. A time domain transient and its corresponding mass spectrum produced by performing a Fourier transform.

ubiquitin, formed by electrospray ionization.) The Fourier transform of any portion of this transient would show the same group of ions. Although all the mass-to-charge information is present in a short segment of the transient, there is an advantage to measuring the full duration of the signal. Mass resolution improves in direct proportion to the length of the transient that is recorded. The maximum resolution that can be achieved for a data set is shown in Eqn (5), where R is resolving power, f_c is the cyclotron frequency and T is the duration of a transient.

The dependence of resolution on transient duration is illustrated in Fig. 10, which compares the results of performing a Fourier transform on the full 1.2 s transient of Fig. 10 with a transform of the first 0.15 s of the same transient. The resolution obtained from the shorter transient is clearly much lower than that obtained from the full transient. Thus higher resolution is achieved by

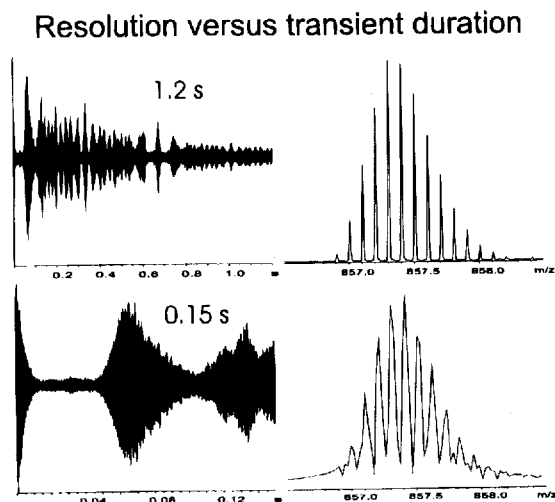


Figure 10. An illustration of the relationship between the length of the transient that is examined and the resolution that can be achieved. The top mass spectrum is obtained from a 1.2 s transient and exhibits a resolution of $\sim 90\,000$ (FWHM). The bottom mass spectrum is obtained from the first eighth of the same transient (150 ms) and exhibits eight times lower resolution, $\sim 12\,000$ (FWHM).

obtaining a longer transient signal. There is a physical limitation to the length of the transient that can be acquired. The amplitude of the transient signal decays with time as collisions between the ions and neutrals in the analyzer cell destroy the coherence of the ion packet. Thus, FTMS works best at ultra-high vacuum, where the collision frequency is lowest. At 10^{-10} Torr, transients of 60 s or longer have been obtained, demonstrating mass resolution in excess of 10^6 , much higher than can be obtained with any other type of mass spectrometer. An example of such ultra-high resolution is shown in Fig. 11, which shows a 1.5×10^6 resolution (FWHM) obtained near m/q 1100, with a 52 s transient from MALDI of the peptide gramicidin S.

$$R = \frac{f_c T}{2} \quad (5)$$

Tandem mass spectrometry

The experimental sequence in Fig. 7 executes a simple mass measurement. More complex experiments are performed by adding additional events to the experimental sequence. With FTMS, experimental sophistication can be achieved through the design of complex experimental sequences rather than through the modification of the instrument's hardware. This is an advantage compared with most other types of mass spectrometer for which expensive modifications of the design of the hardware are usually required to perform experiments that are more elaborate than simple mass measurement. For example, with magnetic sector or quadrupole mass spectrometers, performing a tandem mass spectrometric (MS/MS) experiment, requires additional mass analyzers. With FTMS, MS/MS is achieved with the same hardware that has been described above to carry out simple mass measurement. The experimental sequence is expanded to include pulse sequences for the mass selection of a precursor ion and for its dissociation.

Several types of events can be added to an experimental sequence to perform a wide variety of functions.

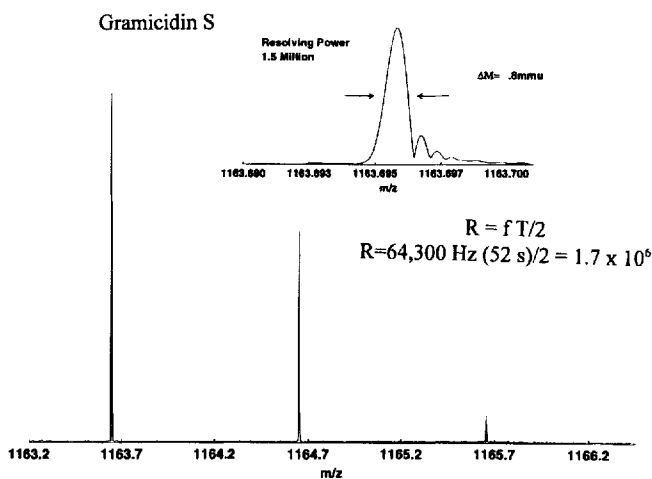


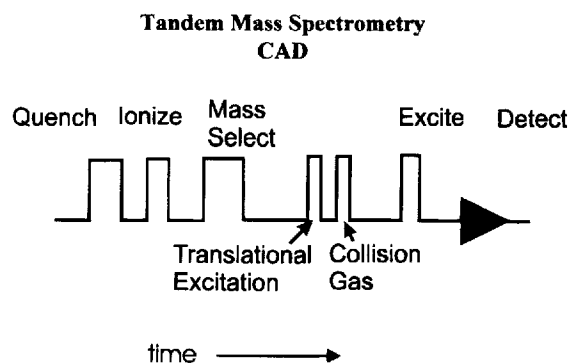
Figure 11. An illustration of ultra-high resolution obtained by MALDI/FTMS of gramicidin S. The base peak exhibits mass resolution of 1.5×10^6 . The inset shows a 10 μ expansion of the region around the base peak.

Different types of excitation waveforms can be applied to the cell plates to manipulate ions in the cell in a mass-selective fashion. Ions of one mass-to-charge ratio can be left at the center of the cell while others are excited to a larger cyclotron radius and still others are ejected from the analyzer. Other excitation events can be used to push ions dispersed throughout the analyzer cell back to its center. The trapping voltages can be changed during the course of an experiment to capture ions that are formed outside the analyzer cell (gated trapping), or to allow some of the ions present in the cell to escape (suspended trapping).⁶⁸ Gaseous samples can be introduced at various points of the experimental sequence through electronically controlled pulsed valves to collisionally activate ions,⁶⁹ to thermalize ions⁷⁰ or to undergo chemical reactions with the ions.⁷¹ Pulsed lasers can be triggered during the experimental sequence to form ions⁷² or to photodissociate mass-selected ions.⁷³ By combining these and other events into an experimental sequence, the basic FTMS instrument can perform a variety of tasks.

Collisionally activated dissociation

An example of an MS/MS experimental sequence is shown in Fig. 12. The sequence begins with a quench pulse and an ionization pulse. Once ions have been formed and trapped in the analyzer cell, mass selection of the precursor can take place. This is achieved by ejecting from the cell all ions of higher and lower masses than the precursor through the application of suitable excitation pulses with the appropriate frequencies and amplitudes. After ejection of the selected ions, the precursor is driven into a larger radius orbit to increase its kinetic energy.

The relationship between kinetic energy and radius is easily derived from the cyclotron equation and is shown in Eqn (6), where E is kinetic energy and r is the cyclotron radius. As can be seen, the kinetic energy increases as the square of the cyclotron radius. An ion of m/q 1000 with one positive charge, at 7 T, excited to a 2 cm



Many types of mass selection and excitation:
Chirp, Burst, SWIFT, Tailored Waveforms, SORI, RAM, MECCA

Figure 12. An experimental sequence that can be used for tandem mass spectrometry, showing the basic steps of ion formation, isolation, collisional dissociation and detection. Mass selection and precursor translational excitation are shown as separate events in this sequence, but can occur at the same time if SWIFT is employed.

radius orbit will have 950 eV of kinetic energy. The mass-selected, kinetically excited ion is then allowed to undergo collisions with a gas admitted through a pulsed valve. The resulting collisions lead to the decomposition of the ion. Provided that the pulse of gas pressure is not too high, the extent of collisionally mediated radial diffusion is sufficiently low so that ions are not lost from the cell. After this process, the resulting product ions are excited and detected as described above.

$$E = \frac{q^2 B^2 r^2}{2m} \quad (6)$$

One drawback to the MS/MS experiment presented above is that product ions are formed away from the center of the cell. Ions that are far from the center of the cell cannot be detected with the same efficiency or resolution as ions that are centered in the analyzer cell. Other schemes for collisionally activated decomposition have been developed for the FTMS instrument to overcome this limitation. Sustained off-resonance excitation (SORI)⁷⁴ has been particularly useful for the dissociation of multiply charged ions formed by electrospray ionization.⁷⁵ With SORI, a low-amplitude r.f. excitation is applied to the precursor ion at a frequency that is slightly off-resonance from the cyclotron frequency. The excitation frequency is alternately in-phase and out-of-phase with the ion, causing its cyclotron orbit to expand and shrink repeatedly. The amplitude of the excitation is kept low so that the ion never goes far from the center of the cell. While this excitation is applied, the pressure is raised in the analyzer cell by admitting a collision gas through a pulsed valve. Under these conditions, the precursor ion undergoes many low-energy collisions, which slowly activate the ion until it reaches its threshold for dissociation. The product ions are formed near the center of the analyzer cell and therefore can be efficiently detected.

Modes of excitation

Many types of excitation waveforms can be used for MS/MS experiments. Ions are excited to a larger cyclotron radius or ejected from the cell when their cyclotron frequency is in resonance with the frequency of the excitation signal. Ions can be ejected with an r.f. burst, an excitation waveform with a fixed frequency. This is particularly useful if only ions of one mass-to-charge need to be ejected. To eject a range of masses, an r.f. chirp can be used that is higher in amplitude or longer in duration than the chirp that is used for ion detection. However, the r.f. chirp and r.f. burst suffer from poor mass resolution in ejecting ions. The reason for this can be seen in Fig. 13, which shows a r.f. chirp in the time domain and its amplitude versus frequency representation or power spectrum, obtained by taking the Fourier transform of the chirp waveform. The power that is delivered to the ions is not evenly distributed over the desired excitation range, so that all ions are not excited to the same cyclotron radius. In addition, the edges of the frequency spectrum slope considerably, so that it is difficult to eject ions of one m/q without exciting ions that are close in mass.

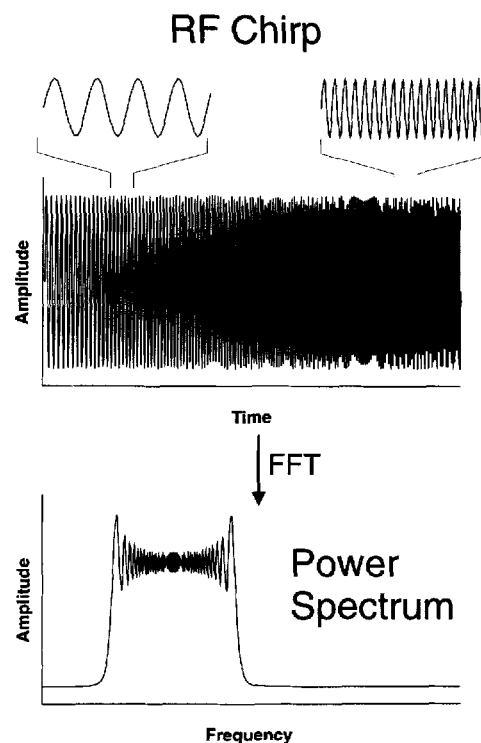


Figure 13. A r.f. chirp and its power spectrum. Power is observed to be unevenly distributed across the spectrum and drops off slowly outside the region of excitation.

In the mid 1980s, Marshall *et al.*⁷⁶ proposed a method to produce the optimal excitation waveform characteristics. This is accomplished by first specifying the desired frequency domain characteristics and then taking the inverse Fourier transform of the frequency spectrum to produce a time domain excitation signal. The basis of this excitation method, called stored waveform inverse Fourier transform, or SWIFT, is illustrated in Fig. 14. The desired waveform for ion isolation and collisional dissociation, displayed at the top of the figure, provides sufficient excitation to eject the ions on the low-frequency side and high-frequency side of the precursor. In addition, the precursor ion, with a cyclotron frequency in between the two ranges that are to be ejected, will receive excitation to drive it into a large-radius orbit without ejecting it, by applying half the power that is applied to the ions that are ejected. The inverse Fourier transform is applied to the specified frequency spectrum to provide a time domain waveform, shown at the bottom of the figure, that can be amplified and applied to the excitation plates of the analyzer cell. The Fourier transform of the excitation waveform returns the original frequency spectrum with sharp frequency cut-offs and uniform power distribution over the specified frequency ranges. The SWIFT waveform simultaneously excites all ions in the specified mass ranges. In the example above, isolation of the precursor and excitation for collisional dissociation occur at the same time.

Quadrupolar excitation

In addition to excitation events that drive ions away from the center of the cell, there is also an excitation

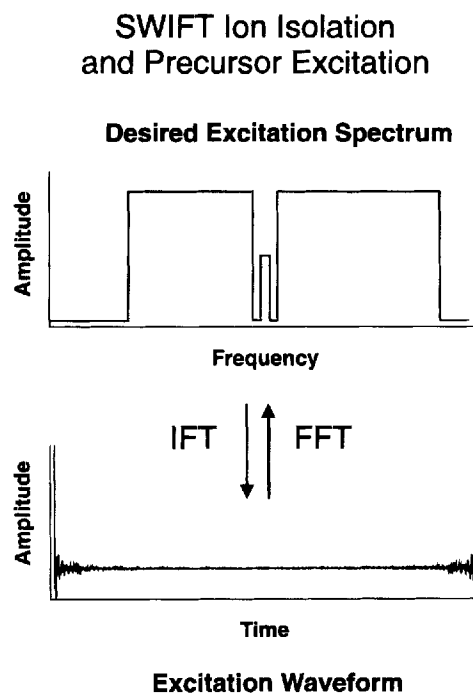


Figure 14. An illustration of the principles of SWIFT excitation. A frequency spectrum is defined at the top. Its corresponding Fourier transform, the SWIFT waveform, is shown at the bottom. Excitation with the SWIFT waveform will apply power as specified in the frequency spectrum.

event that can be used to bring ions back to the center of the cell. This is accomplished by a method called quadrupolar excitation. As shown in Fig. 6, an ion that undergoes many collisions will undergo radial diffusion and ultimately be lost from the analyzer cell. Radial diffusion of an ion comes about from the collisionally induced expansion of its magnetron orbit. In 1991, it was demonstrated that cyclotron and magnetron motion will periodically interconvert when an ion is excited at its cyclotron frequency by an electric field with a quadrupolar symmetry.⁷⁷ If an ion is exposed to a high pressure of a collision gas while it undergoes quadrupolar excitation, then cyclotron motion will dampen more rapidly than magnetron motion. This comes about because an ion's collision frequency is proportional to its velocity and ions have a higher velocity when they undergo cyclotron motion than the much lower frequency magnetron motion. Removing energy from cyclotron motion causes an ion to relax to the center of its orbit. Thus when quadrupolar excitation is applied, collisions with neutrals cause ions to return to the center of the cell, as shown in Fig. 15. This process is called axialization.

Quadrupolar excitation is achieved by applying the same phase of the excitation signal to opposite pairs of plates, as shown in Fig. 15. This stands in contrast to dipolar excitation, in which opposite phases of a waveform are applied to the two excitation plates to drive ions into an orbit suitable for image current detection. As originally proposed, quadrupolar excitation is achieved by applying the r.f. signal to the four plates that are used for normal excitation and detection, with one phase of the signal applied to the excitation plates and the opposite phase applied to the 'detection' plates.

Quadrupolar excitation can be more easily achieved by applying only one phase of the r.f. signal to the two excitation plates and leaving the detection plates at ground potential.⁷⁸ This simplifies the application of quadrupolar excitation, as the second pair of plates do not have to be switched between excitation and detection functions. Many collisions are required to axialize an ion. This is achieved by the introduction of a collision gas through a pulsed valve, to raise the analyzer cell to a relatively high pressure of 10^{-5} Torr or higher. The collision gas is then rapidly pumped away, so that dipolar excitation and detection can occur at low pressure.

Quadrupolar excitation, like dipolar excitation, is a resonant process; the r.f. excitation is applied at the cyclotron frequency of the ions of interest. When a collision gas is introduced, the ions that are in resonance with the excitation field are axialized, while the rest of the ions undergo radial diffusion. Thus quadrupolar excitation can be used to retain in the analyzer cell ions of a single mass-to-charge ratio, while the others are ejected. Like dipolar excitation, quadrupolar excitation can be achieved for a range of masses simultaneously by using a r.f. chirp or a SWIFT waveform to excite ions over a range of frequencies.^{79,80} White noise can also be used as a quadrupolar excitation signal to permit axialization over a wide mass range.^{81,82}

The axialization of ions complements the many types of dipolar excitation that are used to increase mass selectively the radius of an ion's cyclotron orbit. With these tools, ions can be pushed toward the edge of the analyzer cell and later returned to the center. Quadrupolar excitation can be used to trap ions in the cell while they sustain thousands of collisions. When ions undergo quadrupolar excitation while at the center of the analyzer cell, they experience thermal collisions which can be used to remove excess internal energy. This has been used to thermalize excited state ions, in order to study their ground-state gas-phase chemistry.⁸³ Axialization is also used to enhance the signal-to-noise ratio in a mass spectrum by allowing the same set of ions to be detected many times. As with other analytical instruments, the signal-to-noise ratio increases as the square root of the number of scans that are averaged together. Until recently, signal averaging was accomplished by repeating an entire experimental sequence, including the quench and ionization events. This means that after a detection event, the ions which remained in the analyzer cell were discarded. Given the non-destructive detection of the FTMS instrument, it seems logical that after detection, the ions could be re-used for further detection events. With quadrupolar excitation/axialization, such remeasurement is achieved.⁸⁴ Remeasurement reduces the detection limits of the FTMS instrument and has been used to demonstrate attomole detection limits for ions formed by MALDI.⁸⁵

RESOLUTION AND MASS ACCURACY

FTMS is capable of achieving much higher mass resolution than any other type of mass spectrometry. It also is capable of providing mass accuracies of the order of a few ppm over a fairly wide m/q range. Although

mass accuracy may improve with increased resolution, this is not always guaranteed in FTMS. There are a number of effects which can limit mass accuracy while still permitting high resolution. Some practical considerations in achieving high resolution and high mass accuracy are presented below.

Heterodyne detection

High mass resolution is achieved by recording a long time domain image signal, or transient. One factor that limits the length of the transient that can be recorded is pressure-induced damping, which was described above. The image signal can persist for tens of seconds or even minutes when the pressure in the analyzer cell is below 10^{-9} Torr. For such long signals, the length of the recorded transient is limited by the amount of memory in the transient digitizer that is available for acquiring the data and the amount of computer memory that is available for performing the Fourier transform of the data. For many modern data systems, 10^6 data points is an upper limit to the size of the data sets that is recorded and processed. Less than a decade ago, the upper limit was 64 000 data points. The number of data points, N , that are required to record a transient of duration T depends on the rate at which data are sampled, S , according to the equation $T = N/S$. The Nyquist criterion states that to digitize a signal without introducing artifacts, the sampling rate, S , must be at least twice the highest frequency that is recorded. Since mass-to-charge ratio is inversely proportional to cyclotron frequency, the sampling rate is determined by the lowest mass ion that is recorded. For example, to record a mass spectrum from m/q 500 to 5000 with a 7 T FTMS instrument, the highest cyclotron frequency that could be recorded is ~ 215 kHz, corresponding to m/q 500. The sampling rate in this case would have to be no smaller than 430 kHz. If the sampling rate is 500 kHz, then 500 000 data points will be recorded per second. A very large data set of 10^6 data points will be recorded in only 2 s. According to Eqn (5), a 2 s transient corresponds to 200 000 resolution for an m/q 500 ion at 7 T and 20 000 resolution for an m/q 5000 ion.

In order to record a longer transient and thereby obtain higher resolution, heterodyne detection can be used to allow sampling to occur at a lower rate. The principle of heterodyne detection, also called narrow-band detection or mixer mode, is illustrated in Fig. 16. With heterodyne detection, the image signal is multiplied by a reference frequency that is close to that of the signal of interest. Multiplying two sinusoidal signals together produces a composite signal that contains components with frequencies equal to the sum and difference of the frequencies of the two original signals. The high-frequency component can be removed with a low-pass filter to leave the difference frequency. For example, an m/q 510 ion has a cyclotron frequency of 210 kHz. If this signal is multiplied by a reference signal of 200 kHz, then the difference frequency is only 10 kHz and can be sampled at a rate of 20 kHz. At this rate, a 50 s transient could be recorded with 10^6 data points, with a consequential improvement in resolution of 25 over the direct acquisition with a sampling rate of

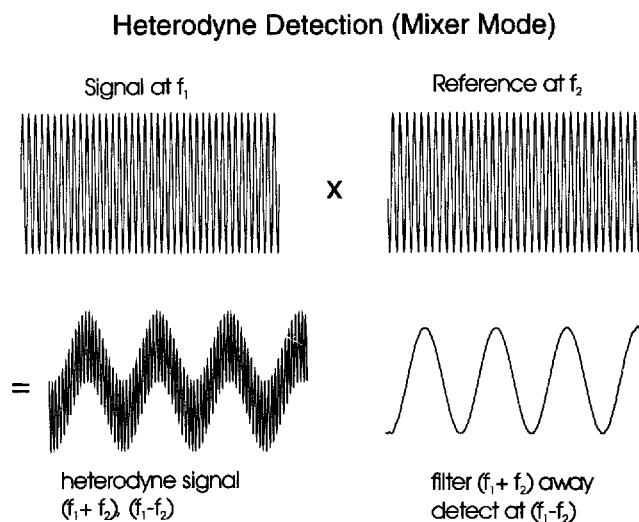
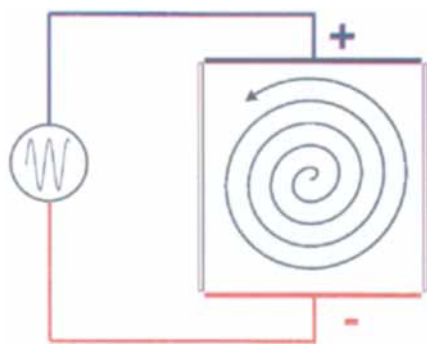


Figure 16. An illustration of the principles of heterodyne detection. The signal produced by the image current (top left) is multiplied by a reference frequency (top right) that is close to, but not equal to, the frequency of the signal. The resultant signal (bottom left) has two components, a sum and a difference frequency. The high-frequency component is removed with a low-pass filter to leave the low-frequency component (bottom right), which can be detected by using a substantially lower digitization rate than the original signal.

500 kHz. The Fourier transform of the heterodyne signal for the m/q 510 ion would yield a frequency spectrum with a peak at 10 kHz. This is added to the reference frequency, 200 kHz, to yield the actual cyclotron frequency of 210 kHz. Ions with cyclotron frequencies from 200 to 210 kHz will have difference frequencies between 0 and 10 kHz and can be sampled at 20 kHz. These frequencies correspond to ions of m/q 510–535. As the sampling rate of the heterodyne acquisition decreases, longer transients can be recorded, but the mass range that is observed becomes narrower.

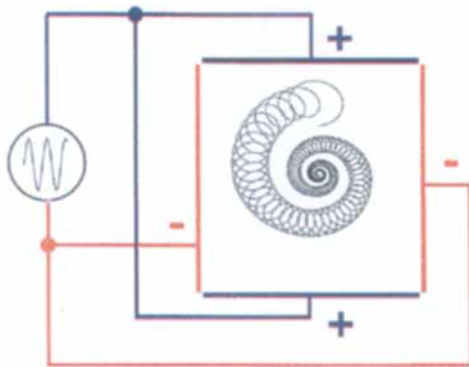
Ion coalescence

A long transient signal is required to obtain narrow peaks in the mass spectrum. However, a narrow peak does not necessarily guarantee high resolution. Resolution is the capability to separate closely spaced peaks. Under some circumstances, peaks that are closely spaced in frequency will coalesce into a single peak. A mechanism that has been proposed for this behavior is a collective motion of ion packets with similar frequencies.⁸⁶ When ions are excited for detection, they first orbit with other ions of the same mass-to-charge ratio, but with time begin to move into synchrony with other ions that have similar cyclotron frequencies, owing to an interaction between electric fields associated with each ion packet. The amount of time that is needed for this collective motion to develop is a function of the number of ions in the cell, the frequency spacing between the ions, the amplitude of the trapping potential, the size of the analyzer cell and the radius of the orbit of the ions.⁸⁷ An example of this behavior is shown in Fig. 17, which shows isotope peaks of an oligomer of polyethylene glycol, which merge as the trapping voltage is increased. This problem is addressed by using lower ion densities and



Dipolar Excitation

$B \otimes$



Quadrupolar Excitation

Figure 15. Comparison of the phase of the voltages applied for dipolar (top) and quadrupolar (bottom) excitation, and their corresponding effect on an ion that is in resonance with the excitation frequency. With dipolar excitation (top), an ion at the center of the cell spirals outwards into a larger radius orbit. With quadrupolar excitation in the presence of a collision gas (bottom), an ion that is displaced from the center of the cell undergoes a trajectory that brings it back to the cell's center.

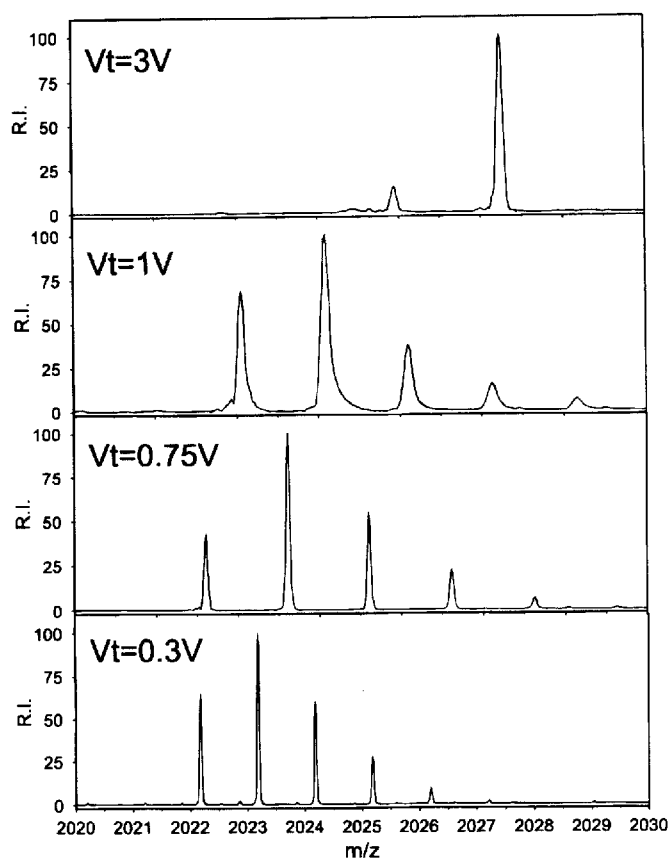


Figure 17. An illustration of the effect of trapping voltage on the coalescence of closely spaced peaks. The signals are from an oligomer of polyethylene glycol, produced by MALDI in a 4.7 T FTMS instrument in the author's laboratory. The expected isotope distribution is observed in the bottom mass spectrum, obtained at 0.3 V trapping potential. As the trapping voltage is increased to 0.75, 1 and 3 V, the peaks are observed to broaden and merge into one main peak. Note that the peaks shift to higher mass (and lower observed cyclotron frequency) as the trapping voltage is raised, consistent with the expected increase in magnetron frequency.

reducing the trapping voltage. In this manner, the FTMS instrument demonstrates excellent resolution. The mass spectrum of insulin has been recorded at over 800 000 resolution.⁸⁸ Closely spaced isotope peaks can be resolved for peptides, for example the $^{13}\text{C}_2$ isotope of [Arg⁸]-vasopressin can be resolved from its ^{34}S isotope, a difference of only 0.04 Da at m/q 1086.

Mass calibration

The methods required to produce high-resolution mass spectra have been presented. The goal of high-resolution mass spectrometry is to make accurate mass measurements. Producing a narrow peak in the mass spectrum does not guarantee the accuracy of the mass measurement. The narrow peaks that are produced by high-resolution FTMS allow the observed frequency to be measured precisely. The observed frequencies must then be converted into a mass-to-charge value by using a calibration equation. As was pointed out earlier, the frequency of the image signal is not precisely equal to the cyclotron frequency but rather is equal to the difference between the cyclotron frequency [Eqn (2)] and the magnetron frequency [Eqn (4)]. The magnetron fre-

quency is independent of mass-to-charge ratio and causes the observed frequency to decrease as the trapping voltage is increased. This behavior is consistent with the picture of the electric field due to the trapping potential, as shown in Fig. 4. As the trapping potential increases, the potential at the center of the analyzer cell increases, which increases the radially repulsive electric field. This field produces a force which drives ions away from the center of the cell, thus opposing the magnetic force that causes ions to undergo cyclotron motion. The result is that the effective magnetic force on an ion is reduced by the electric field of the trapping potential, causing cyclotron frequencies to decrease. Calibration of the spectrometer can account for the frequency shift introduced by the trapping electric field. The instrument should be calibrated using the same trapping potential as for data collection, although calibration methods have been proposed which account for the effect of trapping voltage on the measured cyclotron frequency.⁸⁹

The observed frequency can be shifted by the space charge of ions in the analyzer cell. It has been shown that the magnitude of this effect depends upon the radius of the cyclotron orbit during detection. Increasing the radius of the cyclotron orbit causes a decrease in the frequency shift due to space charge. Consequently, it is important that data are collected using the same dipolar excitation conditions as used for mass calibration of the spectrometer. The calibration is more accurate if the number of ions is approximately the same for calibration as for data acquisition. With these factors controlled properly, the FTMS instrument can provide mass measurements with low ppm accuracy, even above m/q 1000.⁹⁰ For example, polymers examined by MALDI/FTMS have been measured with sufficient mass accuracy to determine the elemental composition of their end groups.⁹¹

FUTURE PROSPECTS

The Fourier transform mass spectrometer achieves much higher mass resolution and mass accuracy than any other type of mass spectrometer. These capabilities, which previously have been demonstrated in a few laboratories, are now become more widely applied. One measure of the maturity of this technology is that a number of FTMS instruments are now being used by pharmaceutical and biotechnological firms. The combination of ESI with FTMS seems to be a particularly good match. The m/q of ions formed by ESI (500–2000) falls in a range for which the FTMS instrument is capable of providing particularly good performance. Many examples of high-resolution protein and nucleotide analysis by ESI-FTMS can be found in the literature. MALDI/FTMS has recently demonstrated some spectacular performance, but this combination has not yet become as widespread as the coupling of ESI with FTMS. With recent advances in time-of-flight mass spectrometry, isotopic resolution can be achieved at m/q 5000 and higher with comparatively less complex and less expensive instruments. MALDI/FTMS will nevertheless remain the method of choice for problems that require ultra-high resolution. Distinguishing the components of complex mixtures benefits from high-

resolution mass spectrometry. The analysis of combinatorial peptide libraries and of random polymer molecular mass distributions are two areas where the high resolving power of FTMS is now being applied to answer questions that cannot be resolved by other types of mass spectrometry.

The development of very high-field FTMS instruments promises to raise the level of performance to an even higher plain. Over the next few years, both the National High Magnetic Field Laboratory and Battelle Pacific Northwest National Laboratory will produce FTMS instruments with magnetic field strengths of 12 T or higher. Not only will mass resolution and mass accuracy improve with these instruments, but also the mass range to which these high-performance capabil-

ities can be applied will increase. While research in FTMS has focused to date on advancing the technology and developing a firmer understanding of the underlying principles, the future of FTMS will be the widespread application of this high-performance method to complex problems in biological and material science.

Acknowledgements

The author is grateful for generous financial support from the National Science Foundation (CHE-9412334 and BIR-9413918). He thanks the members of his research group who helped to prepare this paper: Michael Easterling, Keith Johnson, Shubhada Kulkarni, Todd Mize, Kristi Taylor and Gary Dent.

REFERENCES

- J. A. Loo, J. P. Quinn, S. I. Ryu, K. D. Henry, M. W. Senko and F. W. McLafferty, *Proc. Natl. Acad. Sci. USA* **89**, 286 (1992).
- B. E. Winger, S. A. Hofstadler, J. E. Bruce, H. R. Udseth and R. D. Smith, *J. Am. Soc. Mass Spectrom.* **4**, 566 (1993).
- C. Koster, J. A. Castoro and C. L. Wilkins, *J. Am. Chem. Soc.* **114**, 7572 (1992).
- Y. Z. Li, D. P. Little, H. Koster, R. L. Hunter and R. T. McIver, *Jr, Anal. Chem.* **68**, 2090 (1996).
- S. C. Beu, M. W. Senko, J. P. Quinn and F. W. McLafferty, *J. Am. Soc. Mass Spectrom.* **4**, 190 (1993).
- J. Yao, M. Dey, S. J. Pastor and C. L. Wilkins, *Anal. Chem.* **67**, 3638 (1995).
- S. A. Hofstadler, E. Schmidt, Z. Guan and D. A. Laude, *J. Am. Soc. Mass Spectrom.* **4**, 168 (1993).
- I. J. Amster, J. A. Loo, J. J. P. Furlong and F. W. McLafferty, *Anal. Chem.* **59**, 313 (1987).
- J. A. Loo, E. R. Williams, I. J. Amster, J. J. P. Furlong, B. H. Wang and F. W. McLafferty, *Anal. Chem.* **59**, 1880 (1987).
- C. H. Watson, C. M. Barshick, J. Wronka, F. H. Laukien and J. R. Eyler, *Anal. Chem.* **68**, 573 (1996).
- S. G. Penn, M. T. Cancilla and C. B. Lebrilla, *Anal. Chem.* **68**, 2331 (1996).
- P. B. Andrade and J. M. Riveros, *J. Mass Spectrom.* **31**, 767 (1996).
- Q. Y. Wu, X. H. Cheng, S. A. Hofstadler and R. D. Smith, *J. Mass Spectrom.* **31**, 669 (1996).
- K. A. Sannes and J. I. Brauman, *J. Phys. Chem.* **100**, 7471 (1996).
- C. J. Cassidy and S. R. Carr, *J. Mass Spectrom.* **31**, 247 (1996).
- S. Campbell, M. T. Rodgers, E. M. Marzluff and J. L. Beauchamp, *J. Am. Chem. Soc.* **117**, 12840 (1995).
- C. Q. Jiao, D. R. Ranatunga and B. S. Freiser, *J. Phys. Chem.* **100**, 4755 (1996).
- R. M. Li, R. L. Smith and H. I. Kentamaa, *J. Am. Chem. Soc.* **118**, 5056 (1996).
- Q. Z. Chen, K. Cannell, J. Nicoll and D. V. Dearden, *J. Am. Chem. Soc.* **118**, 6335 (1996).
- T. L. Zhang, L. P. Wang, M. Hashmi, M. W. Anders, C. Thorpe and D. P. Ridge, *Chem. Res. Toxicol.* **8**, 907 (1995).
- M. K. Green, E. Gard, J. Bregar and C. B. Lebrilla, *J. Mass Spectrom.* **30**, 1103 (1995).
- N. G. Alameddin, M. F. Ryan, J. R. Eyler, A. R. Siedle and D. E. Richardson, *Organometallics* **14**, 5005 (1995).
- J. P. Speir and I. J. Amster, *Am. Soc. Mass Spectrom.* **6**, 1069 (1995).
- Y. P. Ho and R. C. Dunbar, *Int. J. Mass Spectrom. Ion Processes* **154**, 133 (1996).
- T. Solouki and D. H. Russell, *Appl. Spectrosc.* **47**, 211 (1993).
- D. M. Peiris, M. A. Cheeseman, R. Ramanathan and J. R. Eyler, *J. Phys. Chem.* **97**, 7839 (1993).
- G. S. Gorman and I. J. Amster, *Org. Mass Spectrom.* **28**, 437 (1993).
- E. O. Lawrence and N. E. Edlefsen, *Science* **72**, 376 (1930).
- H. Sommer, H. A. Thomas and J. A. Hipple, *Phys. Rev.* **76**, 1877 (1949).
- A. G. Marshall, M. B. Comisarow and G. Parisod, *J. Chem. Phys.* **71**, 4434 (1979).
- M. B. Comisarow and A. G. Marshall, *Chem. Phys. Lett.* **25**, 282 (1974).
- M. B. Comisarow and A. G. Marshall, *J. Mass Spectrom.* **31**, 581 (1996).
- V. H. Vartanian, J. S. Anderson and D. A. Laude, *Mass Spectrom. Rev.* **14**, 1 (1995).
- C. Koster, M. S. Kahr, J. A. Castoro and C. L. Wilkins, *Mass Spectrom. Rev.* **11**, 495 (1992).
- M. W. Senko and F. W. McLafferty, *Annu. Rev. Biophys. Biomol. Struct.* **23**, 763 (1994).
- J. T. Brenna, W. R. Creasy and J. Zimmerman, *Adv. Chem. Ser.* **236**, 129 (1993).
- C. L. Holliman, D. L. Rempel and M. L. Gross, *Mass Spectrom. Rev.* **13**, 105 (1994).
- A. G. Marshall and L. Schweikhard, *Int. J. Mass Spectrom. Ion Processes* **118**, 37 (1992).
- A. G. Marshall, *Acc. Chem. Res.* **29**, 307 (1996).
- S. H. Guan, H. S. Kim, A. G. Marshall, M. C. Wahl, T. D. Wood and X. Z. Xiang, *Chem. Rev.* **94**, 2161 (1994).
- M. P. Irion, *Int. J. Mass Spectrom. Ion Processes* **121**, 1 (1992).
- L. S. Sheng, S. L. Shew, B. E. Winger and J. E. Campana, *ACS Symp. Ser.* **581**, 55 (1994).
- G. M. Alber, A. G. Marshall, N. C. Hill, L. Schweikhard and T. L. Ricca, *Rev. Sci. Instrum.* **64**, 1845 (1993).
- D. F. Hunt, J. Shabanowitz, R. T. McIver, Jr, R. L. Hunter, J. E. P. Syka, *Anal. Chem.* **57**, 765 (1985).
- L. H. Wang, L. P. Chibante, F. K. Tittel, R. F. Curl and R. E. Smalley, *Chem. Phys. Lett.* **194**, 217 (1992).
- S. A. Hofstadler, E. Schmidt, Z. Guan and D. A. Laude, *J. Am. Soc. Mass Spectrom.* **4**, 168 (1993).
- J. T. Brenna, W. R. Creasy, W. McBain and C. Soria, *Rev. Sci. Instrum.* **59**, 873 (1988).
- L. C. Zeller, J. M. Kennady, H. Kentamaa and J. E. Campana, *Anal. Chem.* **65**, 2116 (1993).
- A. G. Marshall, presented at the 44th ASMS Conference on Mass Spectrometry and Allied Topics, Portland, OR, 12-16 May 1996, TOA 9:30.
- S. H. Guan and A. G. Marshall, *Int. J. Mass Spectrom. Ion Processes* **146**, 261 (1995).
- J. B. Jeffries, S. E. Barlow and G. H. Dunn, *Int. J. Mass Spectrom. Ion Processes* **54**, 169 (1983).
- T. J. Francl, M. G. Sherman, R. L. Hunter, M. J. Locke, W. D. Bowers and R. T. McIver, Jr, *Int. J. Mass Spectrom. Ion Processes* **54**, 189 (1983).
- E. B. Ledford, D. L. Rempel and M. L. Gross, *Anal. Chem.* **1984**, 2744 (1984).
- C. L. Hendrickson, S. C. Beu and D. A. Laude, *J. Am. Soc. Mass Spectrom.* **4**, 909 (1993).
- G. T. Uechi and R. T. Dunbar, *J. Am. Soc. Mass Spectrom.* **3**, 734 (1992).

56. R. T. McIver, Jr, *Rev. Sci. Instrum.* **41**, 555 (1970).
57. L. Schweikhard, S. H. Guan and A. G. Marshall, *Int. J. Mass Spectrom. Ion Processes* **120**, 71 (1992).
58. D. L. Rempel and M. L. Gross, *J. Am. Soc. Mass Spectrom.* **3**, 590 (1992).
59. P. Kofel, M. Alleman, H. Kellerhals and K. Wancek, *Int. J. Mass Spectrom. Ion Processes* **65**, 97 (1985).
60. J. A. Marto, A. G. Marshall, M. A. May and P. A. Limbach, *J. Am. Soc. Mass Spectrom.* **6**, 936 (1995).
61. R. T. McIver, Jr, R. L. Hunter and W. D. Bowers, *Int. J. Mass Spectrom. Ion Processes* **64**, 67 (1985).
62. M. Dey, J. A. Castoro and C. L. Wilkins, *Anal. Chem.* **67**, 1575 (1995).
63. S. A. Hofstadler, Q. Y. Wu, J. E. Bruce, R. D. Chen and R. D. Smith, *Int. J. Mass Spectrom. Ion Processes* **142**, 143 (1995).
64. L. Tang, R. L. Hettich, G. B. Hurst and M. V. Buchanan, *Rapid Commun. Mass Spectrom.* **9**, 731 (1995).
65. R. C. Beavis and B. T. Chait, *Chem. Phys. Lett.* **181**, 479 (1991).
66. M. B. Comisarow, *J. Chem. Phys.* **69**, 4097 (1978).
67. V. Frankevich, M. Soni, M. Nappi, R. G. Cooks, R. E. Santini and J. W. Amy, presented at the 44th ASMS Conference on Mass Spectrometry and Allied Topics, Portland, OR, 12-16 May 1996, MPD 63.
68. B. T. Cooper and S. W. Buckner, *Org. Mass Spectrom.* **28**, 914 (1993).
69. R. B. Cody and B. S. Freiser, *Int. J. Mass Spectrom. Ion Phys.* **41**, 199 (1982).
70. J. P. Speir, G. S. Gorman and I. J. Amster, *J. Am. Soc. Mass Spectrom.* **4**, 106 (1993).
71. T. J. Carlin and B. S. Freiser, *Anal. Chem.* **55**, 571 (1983).
72. D. A. McCrery, E. G. Ledford, Jr, and M. L. Gross, *Anal. Chem.* **54**, 1435 (1982).
73. G. T. Uechi and R. C. Dunbar, *J. Chem. Phys.* **96**, 8897 (1992).
74. J. W. Gauthier, R. R. Trautman and D. B. Jacobson, *Anal. Chim. Acta* **246**, 211 (1991).
75. M. W. Senko, J. P. Speir and F. W. McLafferty, *Anal. Chem.* **66**, 2801 (1994).
76. A. G. Marshall, T. C. L. Wang and T. L. Ricca, *J. Am. Chem. Soc.* **107**, 7893 (1985).
77. G. Savard, S. Becker, G. Bollen, H. J. Kluge, R. B. Moore, L. Schweikhard, H. Stolzenberg and U. Wiess, *Phys. Lett. A*, **158**, 247 (1991).
78. C. L. Hendrickson, J. J. Drader and D. A. Laude, *J. Am. Soc. Mass Spectrom.* **6**, 448 (1995).
79. Y. Huang, L. Paša-Tolić, S. Guan and A. G. Marshall, *Anal. Chem.*, **66**, 4385 (1994).
80. J. A. Marto, S. Guan and A. G. Marshall, *Rapid Commun. Mass Spectrom.* **8**, 615 (1994).
81. J. A. Bruce, G. A. Anderson and R. D. Smith, *Anal. Chem.*, **68**, 534 (1996).
82. C. C. Pitsenberger, M. L. Easterling and I. J. Amster, *Anal. Chem.*, **68**, 3732 (1996).
83. Q. P. Lei and I. J. Amster, *J. Am. Soc. Mass Spectrom.* **7**, 722 (1996).
84. J. P. Speir, G. S. Gorman, C. C. Pitsenberger, C. A. Turner, P. P. Wang and I. J. Amster, *Anal. Chem.* **65**, 1746 (1993).
85. T. Solouki, J. A. Marto, F. M. White, S. Guan and A. G. Marshall, *Anal. Chem.* **67**, 4139 (1995).
86. J. Y. Huang, P. W. Tiedemann, D. P. Land, R. T. McIver, Jr and J. C. Hemminger, *Int. J. Mass Spectrom. Ion Processes* **134**, 11 (1994).
87. E. N. Nikolaev, N. V. Miluchihin and M. Inoue *Int. J. Mass Spectrom. Ion Processes* **148**, 145 (1995).
88. R. T. McIver, Jr, Y. Li and R. L. Hunter, presented at the 44th ASMS Conference on Mass Spectrometry and Allied Topics, Portland, OR, 12-16 May 1996, WOA 4:50.
89. Y. Z. Li, R. T. McIver, Jr, and R. L. Hunter, *Anal. Chem.* **66**, 2077 (1994).
90. J. Y. Wu, S.T. Fannin, M. A. Franklin, T. F. Molinski and C. B. Lebrilla, *Anal. Chem.* **67**, 3788 (1995).
91. G. J. Vanrooij, M. C. Duursma, R. M. Heeren, J. J. Boon and C. G. Dekoster, *J. Am. Soc. Mass Spectrom.* **7**, 449 (1996).